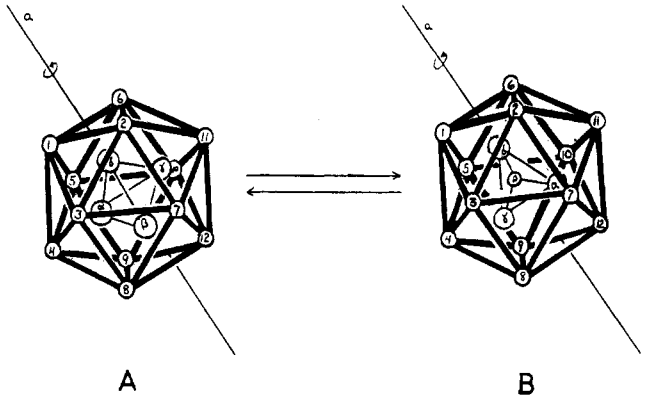

Figure 2. Schematic representation of the structure of $Co_4(CO)_{12}$ showing the 2-fold disorder observed crystallographically. Rotation of the cobalt tetrahedron about the 2-fold axis, *a*, is not sufficient to exchange all 12 carbonyls.

the ^{59}Co–^{13}C dipolar interactions. Thus the spectra at temperatures from −62 to +24 °C probably exhibit some dipolar broadening. Also some selective site exchange may still be taking place at −62 °C.

Although the spectra below 24 °C appear to be consistent with a static molecule, we do not have a satisfactory explanation for the chemical shifts at this time. It is clear that above 24 °C chemical shifts differences as well as dipolar couplings are lost as the signals broaden and finally coalesce at about 52 °C. This can only be explained by a reorientation of the molecule.

The nearly spherical icosahedra of carbonyls in $Co_4(CO)_{12}$ pack very efficiently in the solid. The carbonyl ligands mesh to some extent, and the closest contact between adjacent molecules is between carbonyl oxygens at 2.86 Å.[6a] Thus it seems unlikely that the reorientation involves the rotation of the entire icosahedron. Furthermore, rotation of the entire icosahedron will not make all 12 carbonyl ligands equivalent.

Figure 2 shows a schematic representation of the molecular structure of $Co_4(CO)_{12}$. The numbering scheme is consistent with that given by Johnson and Benfield, who have considered polytopal rearrangements of $Co_4(CO)_{12}$ and its derivatives in solution.[12] In structure A of Figure 2 the cobalt labeled α represents the apical cobalt and is directed at face 4,5,9. Cobalts β, γ, and δ are directed at edges 7,8, 10,11, and 1,2, respectively. The bridging carbonyls are represented by the vertices 3, 6, and 12. Crystallographically the molecule occupies a site of two-fold symmetry. This gives rise to the disorder of the Co_4 tetrahedron. In Figure 2 the observed 2-fold axis is designated *a*; structures A and B are related by the 2-fold axis and represent half-molecules in the crystal structure.

The result of the 2-fold rotation is to interchange carbonyls 1,2, 9,12, 4,11, 5,7, 8,10, and 3,6. Therefore this rotation is not sufficient to interchange all carbonyl sites. However at the temperatures reached in recording the NMR spectra (63 °C), it is possible that all possible orientations of the cobalt tetrahedron are observed, or, in other words, the apical cobalt, α, may be directed at any triangular face in the ligand icosahedron. Reorientation of the tetrahedron to point at an adjacent face requires a rotation of 36°. Adjacent faces, for example, are represented by 4,5,9 and 4,9,8 in structure A.

The activation energy for exchange in the solid, as estimated by the apparent coalescence temperature, ~52 °C, is not significantly greater than observed in solution, where the coalescence temperature may be estimated to be 30 °C.[13,14] Thus it appears that the intramolecular motion described here is only a slightly higher energy process than the fluxional process observed in solution. Also it should be noted that the proposed mechanisms to explain the solution dynamics[12,15] involve expansion of the ligand icosahedron to a cuboctahedron, and this clearly cannot occur in the solid because of the constraints imposed by the lattice.

The reported temperatures in this study were measured by a thermocouple placed in the spinner air stream prior to the sample. Thus these represent an upper limit for the true sample temperature. Also it should be noted that 63 °C is above the reported melting point of $Co_4(CO)_{12}$ (60 °C).[16] Significant line broadening and coalescence, however, occur well below this temperature. Finally, when the rotor was opened after the high-temperature experiment, the sample showed no evidence of having melted; i.e., it was still a polycrystalline solid.

Acknowledgment. We thank the National Science Foundation for support of this work (Grant DMR-8211111).

Registry No. $Co_4(CO)_{12}$, 17786-31-1.

(12) Johnson, B. F. G.; Benfield, R. E. *J. Chem. Soc., Dalton Trans.* **1978**, 1554.
(13) The coalescence temperature for the carbon-13 NMR spectra of $Co_4(CO)_{12}$ is not reported in the literature.[11] However, in the variable-temperature oxygen-17 NMR for $Co_4(CO)_{12}$, coalescence is observed at ca. 57 °C at 54.25 MHz.[14] Because of the greater chemical shift dispersion in oxygen-17 NMR coalescence is observed at a higher temperature.
(14) Aime, S.; Osella, D.; Milone, L.; Hawkes, G. E.; Randall, E. W. *J. Am. Chem. Soc.* **1981**, *103*, 5920.
(15) Cotton, F. A. *Inorg. Chem.* **1966**, *5*, 1083.
(16) Kemmitt, R. D. W.; Russell, D. R. In "Comprehensive Organometallic Chemistry"; Abel, E. W., Stone, F. G. A., Wilkinson, G., Eds.; Pergamon Press: London, 1982; Chapter 34.

Department of Chemistry
Virginia Polytechnic Institute and State University
Blacksburg, Virginia 24061

Brian E. Hanson*
Edward C. Lisic

Received November 21, 1985

Cobalt(II)-Facilitated Transport of Dioxygen in a Polystyrene Membrane

Sir:

Recently there has been considerable interest in the production of oxygen-enriched air by permselective polymer membranes.[1] We report here the enrichment of oxygen in an air sample that is passed through polystyrene which contains a supported Co(II) Schiff base complex as an additive. Subsequent to the start of our work selective transport of gases by metal complexes has been reported in liquid membranes.[2] Our work is novel in concept and mechanism for it incorporates addition of cross linked polymer bound CoSMDPT (SMPDT = *N*,*N*-bis(3-(salicylideneamino)-propyl)methylamine) particles

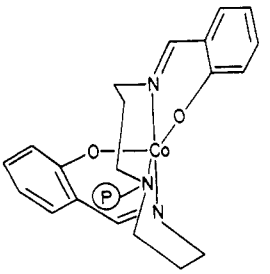

(1) (a) Schell, W. J. *J. Membr. Sci.* **1985**, *22*, 217. (b) Kunitake, T.; Higushi, N.; Kajiyama, T. *Chem. Lett.* **1984**, 717. (c) Masuda, T.; Isobe, E.; Higashimura, T. *J. Am. Chem. Soc.* **1983**, *105*, 7473. (d) Higashimura, T.; Masuda, T.; Okada, M. *Polym. Bull. (Berlin)* **1983**, *10*, 114. (e) Londsdale, H. K. *J. Membr. Sci.* **1982**, *10*, 81. (f) Pusch, W.; Walch, A. *Angew. Chem., Int. Ed. Engl.* **1982**, *21*, 660. (g) Fox, J. L. *Chem. Eng. News* **1982**, *60*, 7. (h) Ward, W. J., III; Browall, W. R.; Salemme, R. M. *J. Membr. Sci.* **1976**, *1*, 99.
(2) (a) Koval, C. A.; Noble, R. D.; Way, J. D.; Lovie, B.; Reyes, Z. E.; Bateman, B. R.; Horn, G. M.; Reed, D. L. *Inorg. Chem.* **1985**, *24*, 1147 and references therein. (b) Roman, I. C.; Baker, I. W. U.S. Patent 4 542 010, 1985.

0020-1669/86/1325-0716$01.50/0

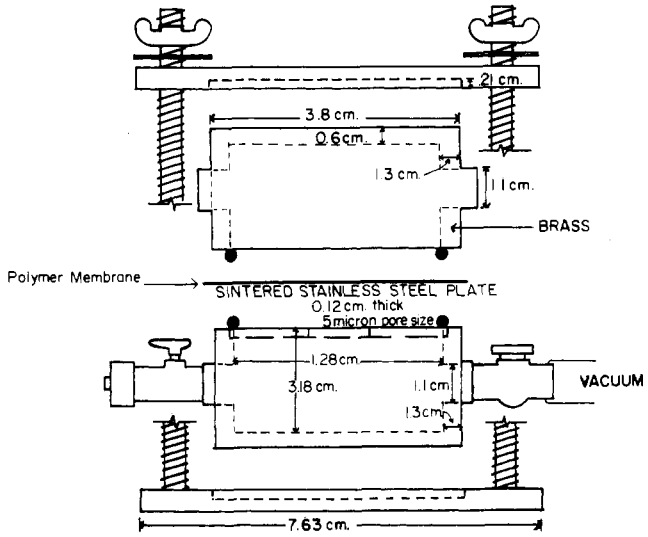

Figure 1. Permeation apparatus.

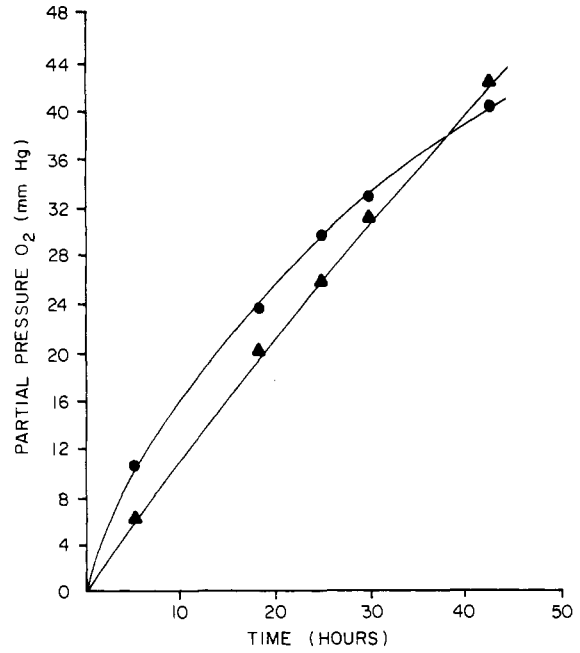

Figure 2. Polystyrene/(Ⓟ)-CoSMDPT film (16.4% by weight of functionalized beads): (●) experimental; (▲) calculated for film without cobalt.

into a solid film of polystyrene. Supported CoSMDPT has been reported to reversibly bind oxygen,[3] and in the solid state we now find that it also enhances the selectivity for oxygen permeation through a polystyrene membrane at low pressures. A manometric technique was employed to obtain the permeation data for flat films. All films were prepared by casting a dispersion of functionalized[3] polystyrene beads (4% cross-linked; 90% substituted) in a dilute polystyrene/toluene solution onto a leveled glass plate and then evaporated to dryness. The resulting membrane was placed in the apparatus shown in Figure 1 with an initial vacuum in the lower chamber and a continuous stream of air passing over the surface of the film in the upper chamber. The pressure differential corresponding to this initial vacuum is the difference between atmospheric pressure and the pressure at $t = 0$ in Figures 2 and 3. The components of the gas mixture permeating through the membrane were analyzed by a thermal conductivity detector (TCD).

(3) Drago, R. S.; Gaul, J.; Zombeck, A.; Straub, D. K. *J. Am. Chem. Soc.* **1980**, *102*, 1033.

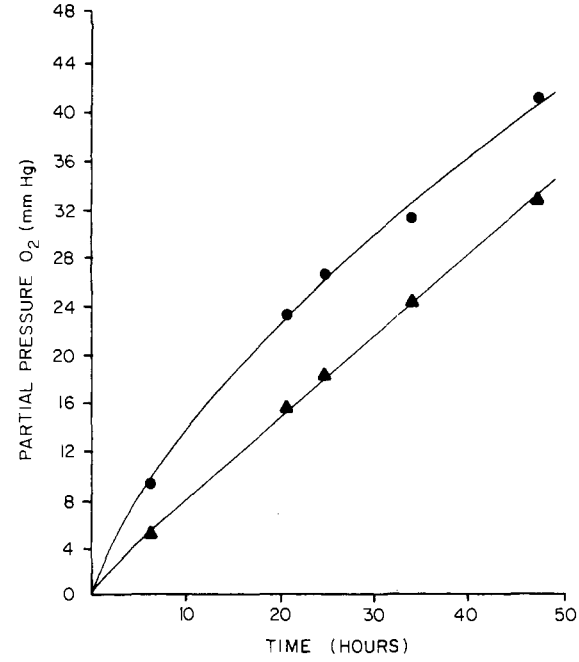

Figure 3. Polystyrene/(Ⓟ)-Co(3,5-Br_2SMDPT) film (18% by weight of functionalized beads): (●) experimental; (▲) calculated for film without cobalt.

We have applied a first-order kinetic treatment to our permeation data:[4]

$$\frac{dP}{dt} = \frac{RTA}{22414V_{cell}} \frac{\bar{P}(P_H - P_L)}{l}$$

$$\int \frac{dP}{P_H - P_L} = \frac{RTA}{22414V_{cell}} \int \frac{\bar{P}}{l} dt$$

with P_H constant

$$d(P_H - P_L) = -dP$$

$$\ln (P_H - P_L) = \frac{-RTA}{22414V_{cell}} \frac{\bar{P}}{l} t + \text{const}$$

where $\bar{P}$ = permeability coefficient (cm^3(STP) cm/(cm^2 s mmHg), l = film thickness (cm), A = film area (cm^2), V_{cell} = volume of lower chamber (cm^3), $P_H - P_L$ = partial pressure difference between the high- and low-pressure sides (mmHg), R = gas constant (6.24×10^4 cm^3 mmHg/(mol K)), T = temperature (K). A plot of ln ($P_H - P_L$) vs. time yields a straight line, indicating a first-order process. The permeability coefficients for oxygen and nitrogen can be obtained from the slope of this line. Over a series of 11 films for polystyrene we find a mean permeability coefficient of 2.6×10^{-10} cm^3(STP) cm/(cm^2 s mmHg) with a standard deviation of $\pm 0.9 \times 10^{-10}$. This permeability coefficient is approximately 1 order of magnitude greater than those previously reported.[6] By virtue of this being a glassy polymer the method of film preparation will greatly affect the transport properties of

(4) This is in preference to the classical solution diffusion model, which employs ϕ, a steady-state permeation rate in the calculation.[5] Often the mass of penetrant is plotted against time and ϕ is the slope of the resulting asymptotic line. The permeability coefficient is

$$\bar{P} = (\phi/A)/(\Delta p/h)$$

where A = area, h = membrane thickness, and Δp is the partial pressure difference across the membrane. For nonswollen rubbery polymers containing no additives this is fine, but for our system this neglects a time period when metal–dioxygen binding is most facile.

(5) Felder, R. M.; Huvard, G. S. *Methods Exp. Phys.* **1980**, *16C*.

(6) (a) Stannett, V. T. *Polym. Eng. Sci.* **1978**, *18*, 1125. (b) Salame, M. *J. Polym. Sci.* **1973**, *41*, 1. (c) Peterson, C. N. *J. Appl. Polym. Sci.* **1968**, *12*, 2649.

the membrane. Our method may allow formation of micropores, and this alone could account for deviation of $\bar{P}_{O_2}$ from reported values. However, systematic errors introduced by the apparatus and the syringing techniques used in sampling may also contribute. Also our permeabilities were determined from a gas mixture rather than a single-component gas permeating through the membrane. Very few studies have been done on the permeation of gas mixtures through glassy polymers. However, in some cases deviations have been observed in permeabilities of pure penetrants vs. those in a mixture.[7] For our purposes, the important point is that consistent values were obtained so that polystyrene and the cobalt-complex-containing membranes can be compared with blanks and the difference in O_2 enrichment attributed to metal-promoted enhanced O_2 permeability.

With use of the permeation data from polystyrene membranes containing various loadings of dispersed functionalized polystyrene beads ($\bar{P}_{O_2} = (5.0 \pm 0.2) \times 10^{-10}$) a partial pressure vs. time curve is measured for an appropriate blank. We note here that a plot of partial pressure of oxygen vs. time for a cobalt (II)-containing membrane compared with the calculated curve for a blank in Figure 2 shows metal-promoted enhanced permeation of oxygen under approximately 16 mmHg of O_2. As the pressure of oxygen increases, we approach the $P_{1/2}$ for the complex and the cobalt is no longer effective for facilitating the transport of oxygen. The thermodynamics of oxygen binding to CoSMDPT in solution have been determined.[8] At 298 K $P_{1/2}$ is calculated to be 6.715×10^3 mmHg. Although comparison of binding constants of supported and solution complexes is not straightforward,[9] supported CoSMDPT in a polymer matrix appears to form a much more stable O_2 adduct than the solution analogue. ESR of the Co–O_2 adduct is still observed even after pumping on the film under a vacuum. When the cobalt is nearly completely oxygenated, O_2 is not removed from the low-pressure side of the film and the driving force for facilitated transfer of O_2 to that surface is removed. The O_2 adduct then functions to inhibit permeation through the film in comparison to the blank by removing free volume. This free volume is generally thought to be the diffusion pathway in the amorphous regions of the polymer. The intersection of the curves in Figure 2 reflects this loss of free volume. The usual mechanism[10] for facilitated transport involves diffusion of the carrier through the film. We have demonstrated facilitated transport in a system where the carrier does not have this mobility.

Substitution of the salicylidene portion of the SMDPT ligand with electron-withdrawing groups should decrease the electron density at the cobalt center as predicted by the spin-pairing model,[11] increasing $P_{1/2}$ for the complex. The oxygen permeation results for a polystyrene film containing polystyrene beads functionalized with the 3,5-Br_2SMDPT analogue are shown in Figure 3. Under approximately 24 mmHg of O_2 the cobalt is enhancing the permeation of oxygen. A slightly higher loading, 18% vs. 16% by weight, coupled with increased reversibility of the complex vastly improves the O_2 enrichment.

The polymer-bound CoSMDPT complexes can be cycled several times, and O_2 enrichment in the permeate gases is noted. However, ESR experiments indicate irreversible oxidation over several days. Studies are anticipated with site isolated silica bound CoSMDPT in order to improve recycling stability. In conclusion, we have demonstrated the enhanced O_2 permeation by polymer-bound CoSMDPT and are currently extending this work to other Co(II) and Fe(II) complexes as well as other polymer systems.

Acknowledgment. We thank the National Science Foundation (Grant No. 8408149) and the U.S. Army (Florida Technology Center) for their support of this research.

(7) Chern, R. T. Ph.D. Thesis, North Carolina State University, 1983, and references therein.
(8) Drago, R. S.; Cannady, J. P.; Leslie, K. A. *J. Am. Chem. Soc.* **1980**, *102*, 6014.
(9) Drago, R. S.; Gaul, J. H. *Inorg. Chem.* **1979**, *18*, 2019.
(10) Way, J. D.; Noble, R. D.; Flynn, T. M.; Sloan, E. D. *J. Membr. Sci.* **1982**, *12*, 239.
(11) Drago, R. S.; Corden, B. B. *Acc. Chem. Res.* **1980**, *13*, 353.

Registry No. Oxygen, 7782-44-7; polystyrene, 9003-53-6; (*N*,*N*-bis(3-(salicylideneamino)propyl)methylamine)cobalt(II), 100313-46-0.

Department of Chemistry
University of Florida
Gainesville, Florida 32611

Russell S. Drago*
Kenneth J. Balkus, Jr.

Received October 11, 1985

Rhodium–Carbon Bond Formation by an Electrochemically Generated Monomeric Rhodium(II) Porphyrin Species

Sir:

The reaction of dimeric rhodium(II) porphyrins with alkyl halides and unsaturated olefins to form a rhodium–carbon bond was first characterized by Ogoshi.[1] These reactions have been postulated to proceed via the monomeric rhodium(II) radical [(P)Rh^{II}·], where P is a porphyrin ligand.[2-4] In this case the initial reaction step is proposed to be homolytic dissociation of the Rh–Rh bond,[2,3] $[(P)Rh]_2 \rightleftarrows [(P)Rh\cdot]$. Monomeric Rh(II) porphyrin radicals have never been isolated, and most studies of rhodium(II) porphyrin reaction chemistry have utilized the dimeric complex. An electrochemically generated Rh(II) radical should show reactivity similar to that of the chemically generated Rh(II) if dimerization can be prevented. This is indeed the case, as presented in this communication.

Recently, we have shown that monomeric Rh(II) porphyrins can be quantitatively and quickly generated by electrochemical reduction of the Rh(III) porphyrin. The lifetime of these radicals depends upon both the temperature and nature of the axial ligands of the initial Rh(III) complex.[5] The electrochemical reduction of $(TPP)Rh(L)_2^+Cl^-$ where L = dimethylamine and TPP is the dianion of tetraphenylporphyrin is reversible at −78 °C and occurs as shown in eq 1. A reversible Rh(III)/Rh(II) reduction is not

$$[(TPP)Rh^{III}(L)_2]^+ \overset{e^-}{\rightleftharpoons} (TPP)Rh^{II}(L)_2 \overset{e^-}{\rightleftharpoons} [(TPP)Rh(L)_2]^- \quad (1)$$

observed for (TPP)Rh(L)Cl at this temperature nor is the first reduction of $(TPP)Rh(L)_2^+Cl^-$ reversible at room temperature, as shown in Figure 1a. This irreversibility is due to a chemical reaction following the generation of Rh(II), which in THF, benzonitrile, or pyridine forms $[(TPP)Rh]_2$.[5]

The reductive behavior of $(TPP)Rh(L)_2^+Cl^-$ in CH_2Cl_2 is different from that in benzonitrile, THF, or pyridine. A chemical reaction follows the first reduction, which, at a scan rate of 0.10 V/s, occurs at $E_p = -1.07$ V vs. SCE in CH_2Cl_2, but no dimer formation is observed in the cyclic voltammograms. Also, the product of the chemical reaction is reversibly reduced at −1.50 V, some 450 mV more positive than the reversible reduction potential of the dimer in benzonitrile. This is illustrated in Figure 1b.

Thin-layer spectroelectrochemistry was used to characterize the first and second reduction of $(TPP)Rh(L)_2^+Cl^-$ in CH_2Cl_2. After the first reduction, the Soret band shifted from 418 to 422 nm and the bands at 528 and 561 nm shifted to 535 and 566 nm. The electronic absorption spectrum of the first reduction product is consistent with formation of Rh(III).[6,7] After the second reduction, the bands at 422 and 535 nm decreased in intensity and a new band appeared at 604 nm, indicative of a porphyrin π-anion radical.

(1) Setsune, J.-I.; Yoshida, Z.; Ogoshi, H. *J. Chem. Soc., Perkin Trans. 1* **1982**, 983.
(2) Wayland, B. B.; Del Rossi, K. J. *J. Am. Chem. Soc.* **1985**, *107*, 7941.
(3) Paonessa, R. S.; Thomas, N. C.; Halpern, J. *J. Am. Chem. Soc.* **1985**, *107*, 4333.
(4) Wayland, B. B.; Woods, B. A. *J. Chem. Soc., Chem. Commun.* **1981**, 475.
(5) Kadish, K. M.; Yao, C.-L.; Anderson, J. E.; Cocolios, P. *Inorg. Chem.* **1985**, *24*, 4515.
(6) Wayland, B. B.; Newman, A. R. *Inorg. Chem.* **1981**, *20*, 3093.
(7) James, B. R.; Stynes, D. V. *J. Chem. Soc., Chem. Commun.* **1972**, 1261.

0020-1669/86/1325-0718$01.50/0